

Supporting Information for:

Solvatochromic AIE luminogens as supersensitive water detectors in organic solvents and highly efficient cyanide chemosensors in water

Yuping Zhang,^a Dongdong Li,^b Yi Li^a and Jihong Yu^{*a}

^a State Key Lab of Inorganic Synthesis and Preparative Chemistry, College of Chemistry, Jilin University, Changchun, 130012, P. R. China.

^b Department of Materials Science, Jilin University, Changchun, 130012, P. R. China.

*Corresponding Author. E-mail: jihong@jlu.edu.cn. Tel: +86-431-85168608. Fax: +86-431-85168608.

Experimental section

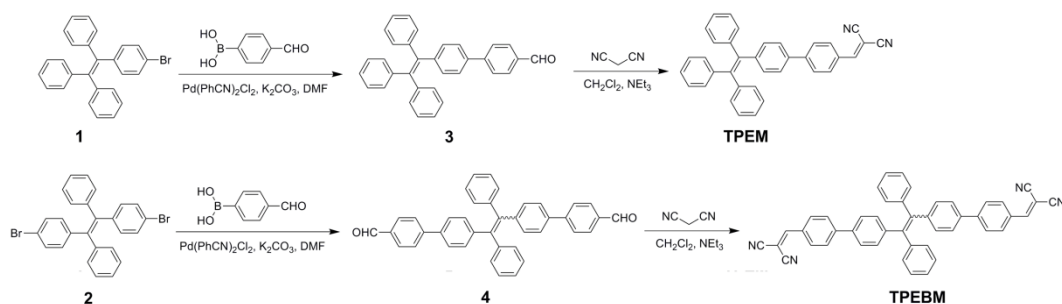
Materials

4-Formylphenylboronic acid (98%) was obtained from Aldrich. Dioxane and tetrahydrofuran (THF) were pre-dried over 4 Å molecular sieves and distilled under nitrogen atmosphere from sodium and benzophenone immediately prior to use. Other solvents were HPLC grade and dried with 4 Å molecular sieves prior to use. Double distilled water from a Millipore Milli-Q plus system was used throughout the work. Cyanide anion was in the form of tetrabutylammonium (TBA) salts, solutions of other anions were prepared from the corresponding potassium salts.

Instrumentation

¹H NMR spectra were recorded by using 300 MHz and 500 MHz spectrometer (tetramethylsilane as the internal standard). ¹³C NMR spectra were recorded at room temperature by using a Varian Mercury spectrometer operating at frequencies 75 MHz. Element analyses (C, H and N) were carried out with a Perkin-Elmer 2400 elemental analyzer. Scanning electron microscope (SEM) images were obtained by using a JEOL JEM-6700F at 3 kV, with the samples sputtered with a layer of platinum (ca. 2 nm thick) prior to imaging to improve conductivity. Transmission electron microscopy (TEM) images were recorded with a Tecnai F20 electron microscope. UV–vis absorption spectra were measured on a Shimadzu 2540 recording spectrophotometer using 2 nm slit width. The fluorescence spectra were collected by using a Shimadzu RF-5301PC spectrophotometer. The fluorescence quantum yield (Φ_F) of the solution was determined by the standard method using quinine sulfate in 0.1 M H₂SO₄ solution as a reference.

Synthetic experimental



Scheme S1 Synthesis route of compounds **TPBM** and **TPEM**.

Synthesis of 4'-((1,2,2-triphenylvinyl)biphenyl-4-yl)carbaldehyde (**3**).

Compounds **1** and **2** were synthesized according to Rathore's method.¹ Pd(PhCN)₂Cl₂ (10 mg) was added into a mixture of compound **1** (0.82 g, 2 mmol), 4-formylphenylboronic acid (0.45 g, 3 mmol) and K₂CO₃ (0.69 g, 5 mmol) in DMF (25 mL) under nitrogen. The reaction mixture was stirred and heated to 80 °C for 48 h. After cooling to room temperature, the solution was poured into the distilled water (200 mL) to precipitate the product. Then, the precipitate was filtered and purified by silica gel column chromatography using petroleum ether/CH₂Cl₂ (4:1 by volume) as the mobile phase. A green solid of compound **3** was obtained (yield: 0.75 g, 86%); ¹H NMR (300 MHz, CDCl₃): δ 10.04 (s, 1H), 7.91 (d, 2H), 7.72 (d, 2H), 7.41 (d, 2H), 7.16-7.03 (m, 17H).

Synthesis of 4',4''-((1,2-diphenylethane-1,2-diyl)dibiphenyl-4-yl)carbaldehyde (**4**).

Compound **4** was synthesized from compound **2** (0.99 g, 2 mmol), 4-formylphenylboronic acid (0.75 g, 5 mmol), K₂CO₃ (1.38 g, 10 mmol), Pd(PhCN)₂Cl₂ (10 mg), and DMF (25 mL). The procedure was similar to that used for compound **3** described above, and a light greenish yellow solid was obtained (yield: 0.84 g, 78%); ¹H NMR (300 MHz, CDCl₃): δ 10.03 (s, 2H), 7.93-7.89 (m, 4H), 7.73-7.70 (m, 4H), 7.46-7.40 (m, 4H), 7.21-7.06 (m, 14H).

Synthesis of 2-((4'-((1,2,2-triphenylvinyl)biphenyl-4-yl)methylene)malononitrile (**TPEM**).

Triethylamine (2 mL) was added to a solution of compound **3** (0.65 g, 1.5 mmol) and malonitrile (0.2 g, 3 mmol) in CH₂Cl₂ (20 mL), and the reaction mixture was

stirred for about 4 h at room temperature. After the solvent was removed under reduced pressure, the residue was purified by using silica gel column chromatography with petroleum ether/CH₂Cl₂ (2:1 by volume) as the mobile phase. A yellow solid was obtained (yield: 0.51 g, 70%). ¹H NMR (500 MHz, DMSO): δ 8.54 (s, 1H), 8.02 (d, 2H), 7.92 (d, 2H), 7.63 (d, 2H), 7.20-7.10 (m, 11H), 7.06-6.99 (m, 6H). ¹³C NMR (75 MHz, DMSO), δ: 160.64, 144.80, 144.00, 143.06, 143.02, 142.97, 141.28, 139.89, 135.91, 131.49, 131.31, 130.70, 130.64, 130.60, 130.24, 127.98, 127.91, 127.80, 127.16, 126.79, 126.67, 126.63, 126.37, 114.39, 113.45, 80.56. Anal. Calcd for C₃₆H₂₄N₂: C, 89.23; H, 4.99; N, 5.78. Found: C, 88.79; H, 5.09; N, 5.65.

Synthesis of 2,2'-(4',4''-(1,2-diphenylethene-1,2-diyl)bis(biphenyl-4',4-diyl))bis(methan-1-yl-1-ylidene)dimalonitrile (TPEBM).

TPEBM was prepared using compound **4** instead of **3** by similar synthetic procedures with the compounds triethylamine (4 mL), compound **4** (0.54 g, 1 mmol), malonitrile (0.33 g, 5 mmol), CH₂Cl₂ (20 mL). An orange-red solid was obtained (yield: 0.36 g, 56%), and its characterization data are given here. ¹H NMR (500 MHz, DMSO): δ 8.54 (s, 2H), 8.01 (t, 4H), 7.93 (d, 4H), 7.69-7.64 (m, 4H), 7.23-7.09 (m, 12H), 7.04 (d, 2H). ¹³C NMR (75 MHz, DMSO), δ : 160.64, 144.78, 143.91, 143.94, 142.93, 142.86, 140.57, 136.03, 131.52, 131.31, 130.75, 130.27, 128.10, 127.93, 127.19, 126.96, 126.79, 126.55, 126.38, 114.38, 113.45, 80.59. Anal. Calcd for C₄₆H₂₈N₄: C, 86.77; H, 4.43; N, 8.80. Found: C, 86.67; H, 4.62; N, 8.64.

References:

1. M. Banerjee, S. J. Emond, S. V. Lindeman and R. Rathore, *J. Org. Chem.*, 2007, **72**, 8054.
2. X. F. Duan, J. Zeng, J. W. Lü, and Z. B. Zhang, *J. Org. Chem.*, 2006, **71**, 9873.

Solvatochromism

The effects of solvents on the emission features can be evaluated by the relationship between the solvent polarity parameter (Δf) and Stokes shift ($\Delta\nu$) of the absorption and emission maxima (Lippert–Mataga equation, eqs 1 and 2)

$$\Delta\nu \equiv \nu_{ab} - \nu_{em} = \frac{2\Delta f}{hca^3}(\mu_e - \mu_g)^2 + const \quad (1)$$

$$\Delta f = \frac{\varepsilon - 1}{2\varepsilon + 1} - \frac{n^2 - 1}{2n^2 + 1} \quad (2)$$

Where, $\Delta\nu$ is the Stokes shift, h is the Planck constant, c is the speed of light, a is the Onsager cavity radius, μ_e and μ_g are the dipolar moments in the excited (e) and ground (g) states, and ε and n are the dielectric constant and refractive index of the solvent, respectively.

The dependency of the emission wavelengths of TPE derivatives on the empirical parameters (E_T^N) of solvent polarity.

$$E_T^N = \frac{E_T(\text{solvent}) - E_T(\text{TMS})}{E_T(\text{water}) - E_T(\text{TMS})} = \frac{E_T(\text{solvent}) - 30.7}{32.4} \quad (\text{TMS} = \text{tetramethylsilane})$$

Preparation of aggregates

Stock solutions (0.1 mM) of TPE-based compounds in DMSO were primarily prepared. An aliquot (0.5 mL) of the stock solution was then transferred to a 10 mL volumetric tube. After the appropriate amount of DMSO was added, water was added dropwise under vigorous stirring to furnish 10 μM solutions with different water contents (0–90 vol %). The absorption and fluorescence spectra of the resultant solutions were performed immediately.

Experimental details for anion sensing

For the UV–vis and fluorescence experiments, the concentration of TPE derivatives solution was 20 μM in CTAB micelles (2 mM). Anion (CN^- , F^- , Cl^- , Br^- , I^- , H_2PO_4^- , AcO^- , HCO_3^- , NO_3^- , NO_2^-) dissolved in the corresponding double distilled water was added. The UV–vis absorption and fluorescence spectra of the samples were recorded after 1 min. ^1H NMR titrations were carried out by using a Bruker AVANCE 500 MHz in DMSO.

The detection limit (DL)

The detection limit is calculated based on the formula $\text{DL} = 3\sigma/|k|$, where σ is the

standard deviation of the blank sample and k is the slope of the calibration curve in the region of low water content or cyanide anions. The standard deviation (σ) was obtained by fluorescence responses (8-times of consecutive scanning on the fluorescence spectrophotometer).

Preparation of the test papers

For the detection of low-level water content in THF and dioxane, the test papers were prepared by immersing filter papers with fixed shape (3.5 cm \times 1.2 cm rectangular) in the stock solutions of TPE derivatives (1 mM) for 10 minutes, and then drying it by exposure to air.

Table S1. Photophysical properties of TPEM and TPEBM in various solvents.

Solvent ^a	Δf	TPEM				TPEBM			
		λ_{abs}^b (nm)	λ_{em}^c (nm)	Stoke's shift (cm ⁻¹)	Φ_F (%)	λ_{abs}^b (nm)	λ_{em}^c (nm)	Stokes shift (cm ⁻¹)	Φ_F (%)
Hex	-0.0010	387	488	5.34799	9	n.d. ^d	n.d.		
Cyc	-0.0016	392	493	5.22623	13	n.d.	n.d.		
Tol	0.0132	392	520	6.27943	11	391	525	6.52783	14
Dio	0.0233	385	527	6.99869	11	385	528	7.03463	12
EA	0.2010	380	553	8.23261	7	380	550	8.13397	7
THF	0.2096	385	565	8.27491	8	388	560	7.91605	8
Chl	0.1479	398	561	7.30032	8	399	554	7.01212	10
DCM	0.2172	390	583	8.48837	3	394	580	8.13933	4
DMF	0.2742	376	595	9.78902	0	384	595	9.23494	0
DMSO	0.2630	385	598	9.25162	0	391	595	8.76872	0
MeCN	0.3055	375	604	10.1103	0	379	597	9.63481	0

^a Abbreviations: Hex, n-hexane; Cyc, cyclohexane; Tol, Toluene; Dio, Dioxane; EA, Ethyl acetate; THF, Tetrahydrofuran; Chl, Chloroform; DCM, Dichloromethane; DMF, Dimethylformamide; DMSO, Dimethyl sulfoxide; MeCN, Acetonitrile. ^b λ_{ab} , absorption maximum, ^c λ_{ex} , emission maximum, ^d n.d., not determined due to the poor

solubility.

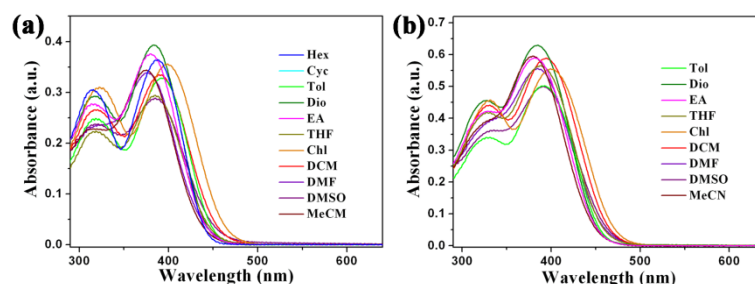


Figure S1. Absorption spectra of (a) TPEM and (b) TPEBM in different solvents. Concentration: 10 μ M.

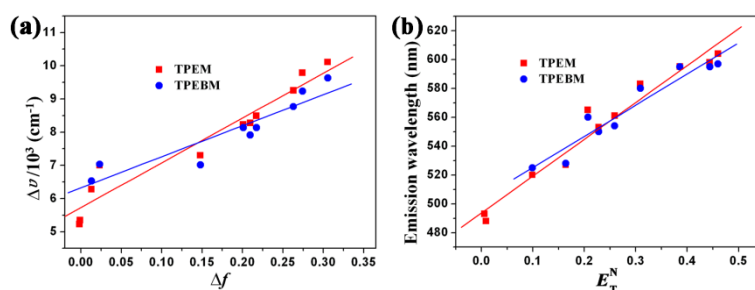


Figure S2. (a) Plot of Stokes shift ($\Delta\nu$) of TPEM and TPEM versus Δf in different solvents. (b) Plot of the fluorescence emission maximum of TPEM and TPEM versus the empirical parameters (E_T^N) of solvent polarity.

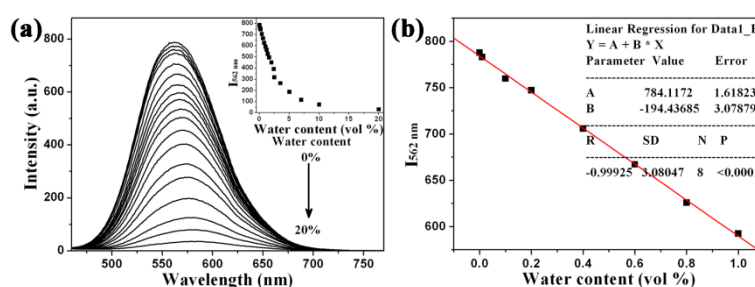


Figure S3. (a) Fluorescence spectra of TPEM in THF solution with increasing amounts of water. Insert: Fluorescence peak intensity at 562 nm of TPEM with increasing water content. (b) Plot of fluorescence intensity change of TPEM versus varied concentrations of H₂O (0–1%, v/v) in THF solution. The detection limit was calculated, giving the result: 0.0056% (63 ppm), $\sigma = 0.3647$. Concentration: 10 μ M; excitation wavelength: 390 nm.

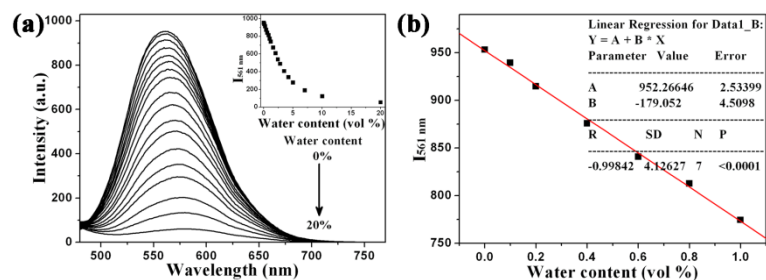


Figure S4. (a) Fluorescence spectra of TPEBM in THF solution with increasing amounts of water. Insert: Fluorescence peak intensity at 561 nm of TPEBM with increasing water content. (b) Plot of fluorescence intensity change of TPEBM versus varied concentrations of H₂O (0–1%, v/v) in THF solution. The detection limit was calculated, giving the result: 0.0097% (109 ppm), $\sigma = 0.5760$. Concentration: 10 μ M; excitation wavelength: 390 nm.

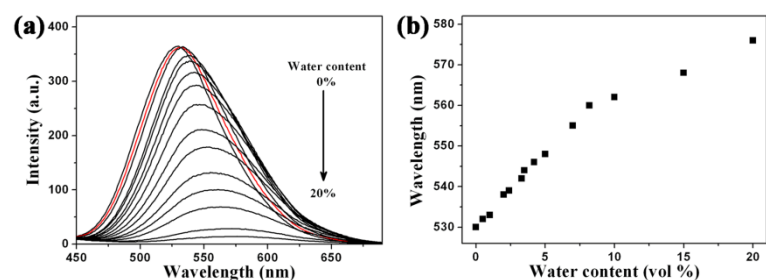


Figure S5. (a) Fluorescence spectra of TPEM in dioxane solution with increasing amounts of water. (b) Plot of emission maximum change of TPEM versus varied concentrations of H₂O (0–20%, v/v) in dioxane solution. Concentration: 10 μ M; excitation wavelength: 390 nm.

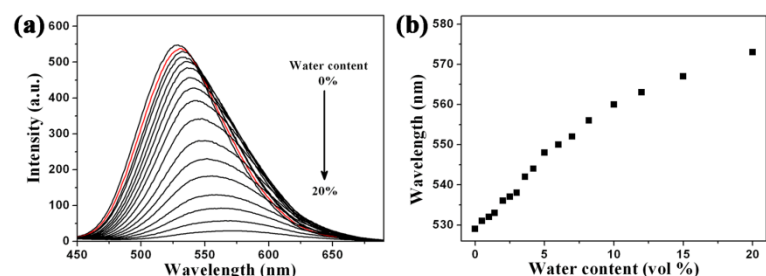


Figure S6. (a) Fluorescence spectra of TPEBM in dioxane solution with increasing amounts of water. (b) Plot of emission maximum change of TPEBM versus varied concentrations of H₂O (0–20%, v/v) in dioxane solution. Concentration: 10 μ M;

excitation wavelength: 390 nm.

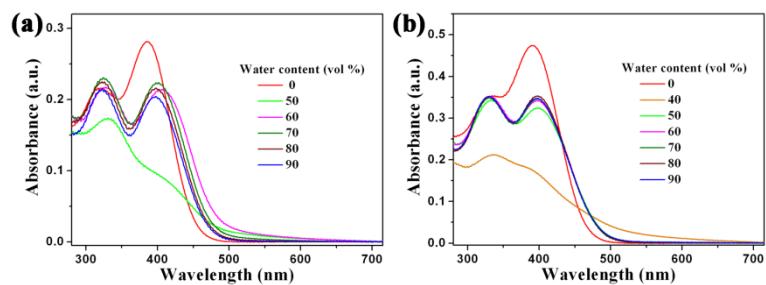


Figure S7. Absorption spectra of (a) TPEM and (b) TPEBM in DMSO/water mixtures with different water contents. Concentration: 10 μ M.

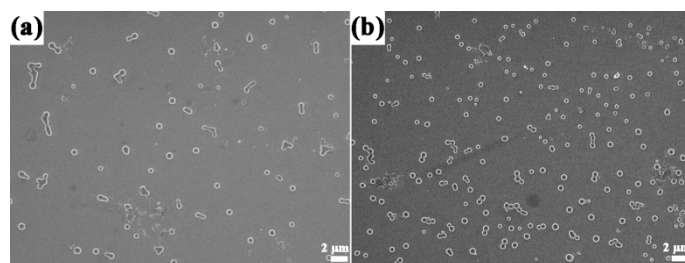


Figure S8. SEM images of (a) TPEM in DMSO/water mixtures with 50% water content and (b) TPEBM in DMSO/water mixtures with 40% water content.

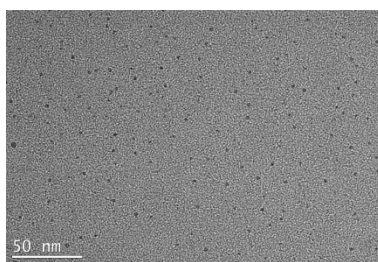


Figure S9. TEM images of TPEBM nanoaggregates obtained from 2 mM CTAB micellar solution.

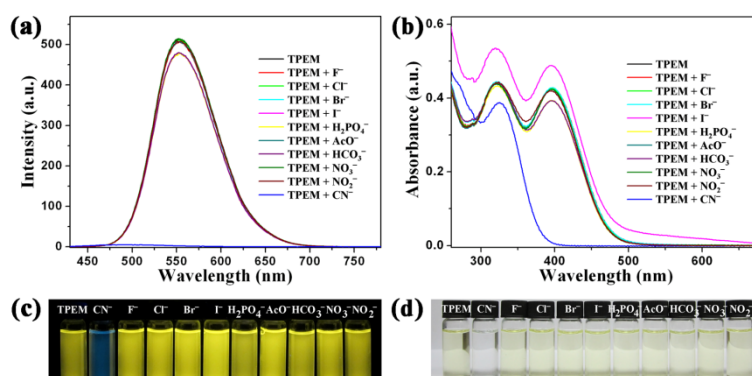


Figure S10. (a) Fluorescence and (b) absorption spectra of TPEM in CTAB micelles (2 mM) upon addition of various anions (CN^- : 5 equiv, other anions: 50 equiv). The corresponding (c) emission and (d) color changes of TPEM in CTAB micelles (2 mM) upon addition of various anions. Concentration: 20 μM ; excitation wavelength: 400 nm.

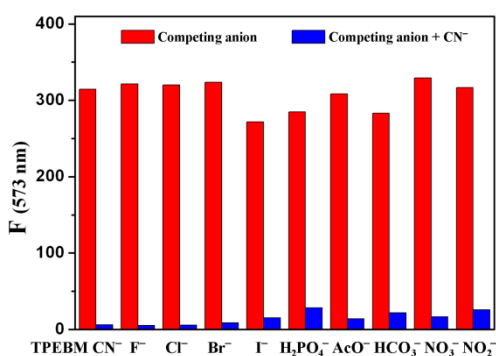


Figure S11. The fluorescence intensity changes at 573 nm of TPEBM (20 μM) in CTAB micelles (2 mM) upon addition of 5 equiv of CN^- and 50 equiv of various interference anions.

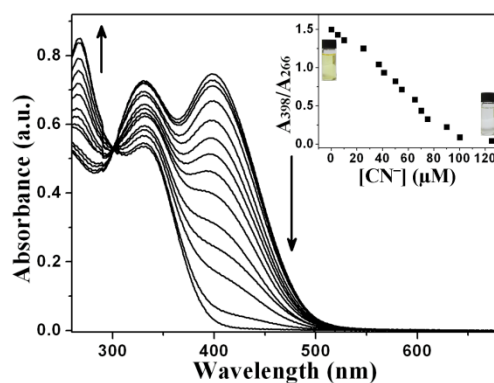


Figure S12. Absorption spectra changes of TPEBM (20 μM) upon the addition of 0–6 equiv cyanide in 2 mM CTAB micellar solution. Insert: plot of absorption intensity ratios (A_{398}/A_{266}) versus concentration of cyanide. Insert: the absorption intensity ratios (A_{398}/A_{266}) as a function of cyanide and images of TPEBM with different amounts of cyanide (left: none; right: 5 equiv cyanide).

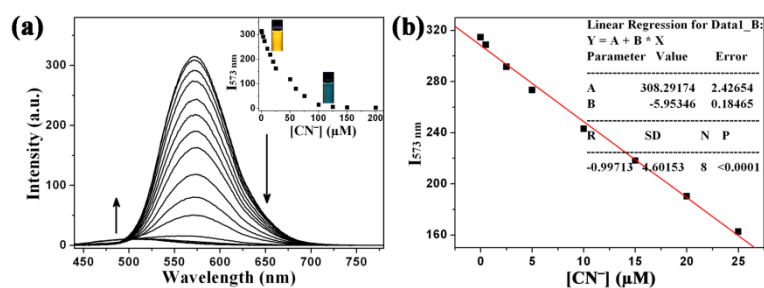


Figure S13. (a) Fluorescence spectra of TPEBM (20 μM) upon the addition of 0–10 equiv cyanide in 2 mM CTAB micellar solution. Insert: Plot of fluorescence intensity at 573 nm versus different cyanide concentration and images of TPEBM with different amounts of cyanide (left: none; right: 5 equiv cyanide). (b) Plot of fluorescence intensity versus cyanide concentration (0–25 μM). The calculated detection limit of probe TPEBM is 0.2 μM ($\sigma = 0.3852$).

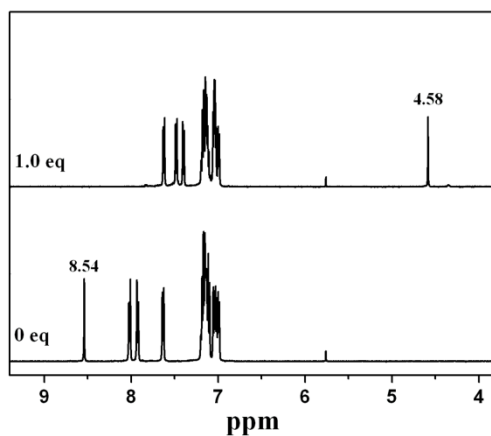


Figure S14. ^1H NMR spectra of TPEM upon the addition of cyanide anion in $\text{DMSO-}d_6$.

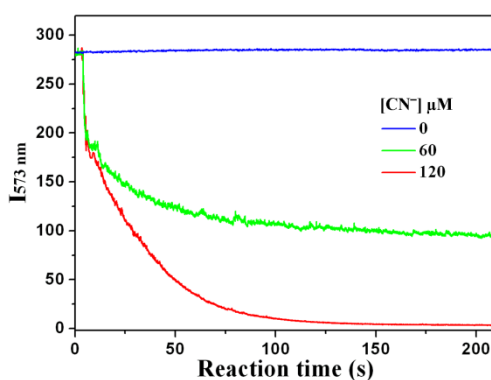


Figure S15. Time-dependent changes in the fluorescence intensity at 573 nm observed from the reaction between TPEBM ($20\ \mu\text{M}$) and different amounts of cyanide anions.

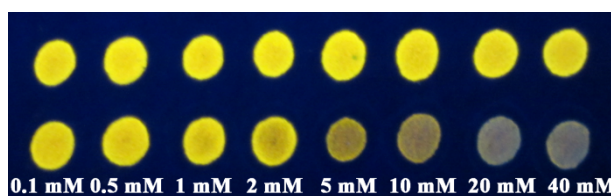


Figure S16. Photographs of test papers containing spots of TPEBM before (upper) and after (bottom) exposure to different concentrations of cyanide anions under irradiation at 365 nm.

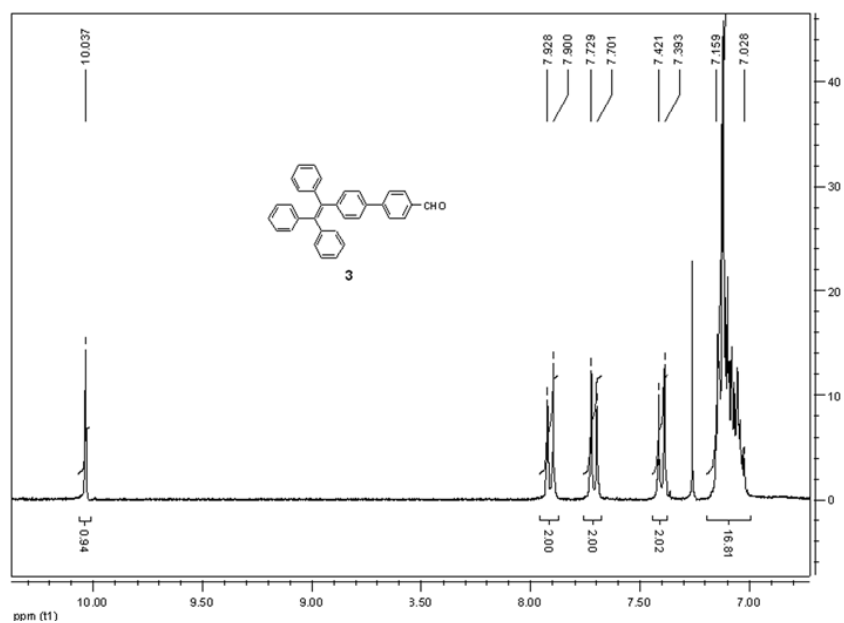


Figure S17. ^1H NMR (300 MHz) spectrum of compound 3.

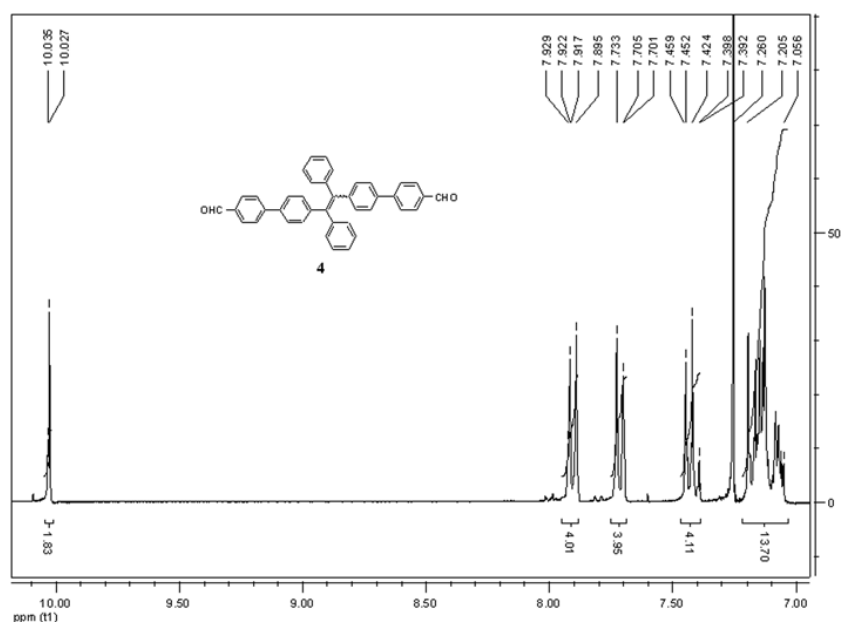


Figure S18. ^1H NMR (300 MHz) spectrum of compound 4.

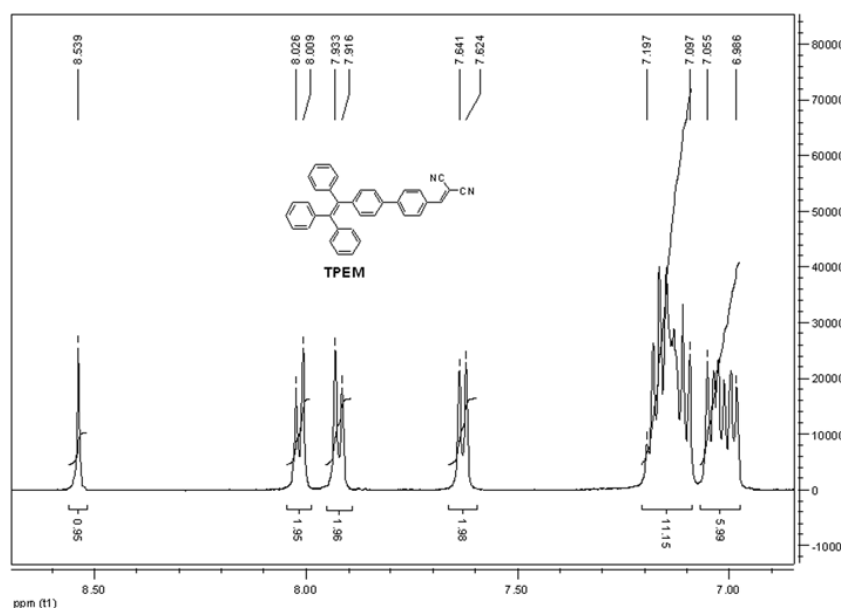


Figure S19. ^1H NMR (500 MHz) spectrum of compound **TPEM**.

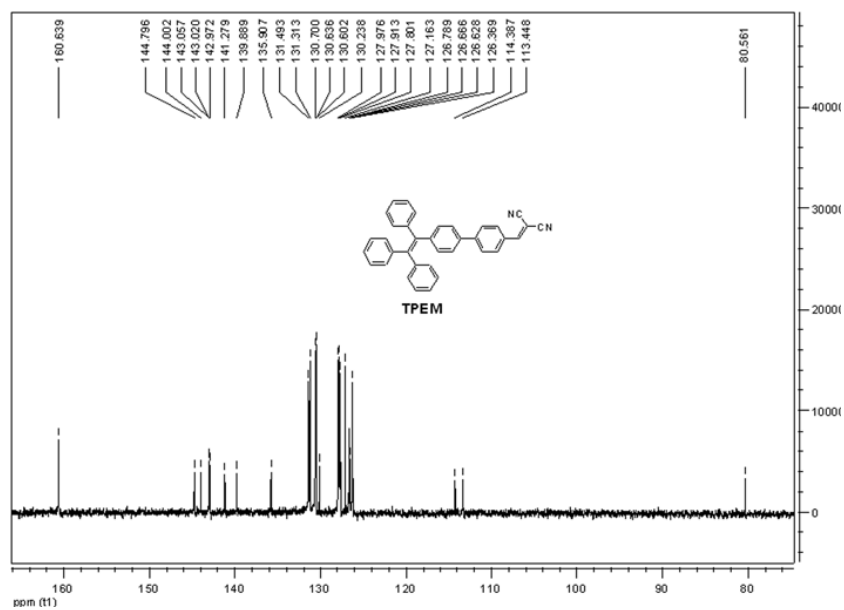


Figure S20. ^{13}C NMR (75 MHz) spectrum of compound **TPEM**.

